

An edited version of this paper was published by [AGU](#).

Global average of air-sea CO₂ transfer velocity from QuikSCAT scatterometer wind speeds

J. Boutin^{1,*}, Y. Quilfen², L. Merlivat¹, J. F. Piolle²

¹ Laboratoire d'Océanographie et du Climat, UMR7159, UPMC, Expérimentation et Approches Numériques, Institut Pierre Simon Laplace, CNRS, Paris, France

² Laboratoire d'Océanographie Spatiale, IFREMER, Brest, France

*: Corresponding author : J. Boutin, email address : jacqueline.boutin@locean-ipsl.upmc.fr

Abstract:

The absolute calibration of the relationship between air-sea CO₂ transfer velocity, k , and wind speed, U , has been a topic of debate for some time, because k global average, $\langle k \rangle$, as deduced from Geochemical Ocean Sections Study oceanic ¹⁴C inventory has differed from that deduced from experimental k - U relationships. Recently, new oceanic ¹⁴C inventories and inversions have led to a lower $\langle k \rangle$. In addition, new measurements performed at sea in high-wind speed conditions have led to new k - U relationship. Meanwhile, quality and sampling of satellite wind speeds has greatly improved. The QuikSCAT scatterometer has provided high-quality wind speeds for more than 7 years. This allows us to estimate the global distributions of k computed using k - U relationships and temperature dependent Schmidt numbers from 1999 to 2006. Given the difficulty of measuring in situ wind speed very accurately, we performed a sensitivity study of the k uncertainty which results from QuikSCAT U uncertainties. New QuikSCAT-buoy U comparisons in the northern Atlantic Ocean and in the Southern Ocean confirm the excellent precision of QuikSCAT U (RMS difference of about 1 m s⁻¹), but it is possible that QuikSCAT overestimates wind speeds by 5%, leading to a possible overestimation of k derived with quadratic relationships by 10%. The $\langle k \rangle$ values obtained with two recent experimental k - U relationships are very close, between 15.9 and 17.9 cm h⁻¹, and within the error bar of k average deduced from the new oceanic ¹⁴C inventory.

32 **1 Introduction**

33 The ocean strongly influences the rate of increase of atmospheric CO₂ linked to CO₂ release
34 into the atmosphere by anthropogenic activities. In fact, since preindustrial times, the ocean
35 has absorbed about one-third of the CO₂ released in the atmosphere by fossil-fuel burning
36 [Sabine *et al.*, 2004]. It is therefore critical for the study of climate that the spatial and
37 temporal distributions of air-sea CO₂ flux be described quantitatively.

38 Locally, air-sea CO₂ flux, F , can be estimated from surface ocean measurements, using a bulk
39 parametrization:

$$40 \quad F = k S \Delta p\text{CO}_2 \quad (1)$$

41 where k is the gas transfer velocity, S is the gas solubility, $\Delta p\text{CO}_2$ is the gradient between
42 atmospheric CO₂ partial pressure and surface ocean CO₂ partial pressure, $p\text{CO}_2$. Hence
43 regional estimates of the air-sea gas flux can be deduced from the integration in space and
44 time of F . The main difficulty in these estimates is linked to our incomplete knowledge of 1)
45 $p\text{CO}_2$ variability and 2) the absolute calibration of the relationship between k , wind speed, U ,
46 and sea surface state. $p\text{CO}_2$ is highly variable in space and time as it is affected by CO₂
47 chemistry in seawater (primarily controlled by sea surface temperature, SST), by ocean
48 physics (advection and diffusion processes), by biological processes and by air-sea exchange.
49 Ocean physics and biological processes are difficult to model, and there exists no simple
50 relationship between $p\text{CO}_2$ and parameters monitored on a global scale. Therefore, current
51 estimates of large scale air-sea CO₂ flux from bulk parametrizations use either the monthly
52 climatology of $p\text{CO}_2$ derived on a global scale from the extrapolation of ship measurements
53 [Takahashi *et al.*, 2002], or empirical relationships established on a regional scale between
54 $p\text{CO}_2$ and satellite-derived parameters (such as SST, SST anomalies and chlorophyll). The
55 latter methodology provides an alternative way to study spatial and seasonal to interannual
56 variability (e.g., in the equatorial Pacific [Boutin *et al.*, 1999a; Etcheto *et al.*, 1999; Feely *et*
57 *al.*, 2002], in the Southern Ocean [Rangama *et al.*, 2005], in the Chile upwelling [Lefèvre *et*
58 *al.*, 2002]).

59 Concerning k , there has been a great deal about the calibration of k - U relationships and the
60 magnitude of its global average. Until recently, the value deduced from global satellite wind
61 speed using experimental k - U relationships (left-hand side of Figure 1) differed by a factor of
62 1.2 to 1.8 from the value deduced by Wanninkhof [1992] from a k - U relationship calibrated
63 with global GEOSECS ¹⁴C oceanic inventories (right-hand side of Figure 1). Recently, new
64 analyses of WOCE measurements revealed that GEOSECS ¹⁴C inventories were high-biased

65 [Peacock, 2004, Key et al., 2004, Naegler and Levin, 2006]. By taking into consideration the
66 new ^{14}C inventories and various inverse models, Krakauer et al. [2006], Naegler et al. [2006],
67 and Sweeney et al. [2007] derive new estimates of global k average that are 9% to 24% lower
68 than the older GEOSECS based average (right hand side of Figure 1).

69 Meanwhile, the QuikSCAT scatterometer has provided unprecedented high-quality satellite
70 wind speeds for more than 7 years. Since its launch, in 1999, it has monitored the surface
71 wind speed at 25 km resolution with almost global ocean coverage every day. In addition,
72 validations with in situ wind speeds indicate that the quality of scatterometer wind speeds is
73 better than that of other remotely sensed wind speeds. Since a good knowledge of both the
74 average and the variability of the wind speed is crucial to constraining k average
75 [Wanninkhof, 2007; Wanninkhof et al., 2002], we can take advantage of this lengthy time
76 series of high-quality wind speeds to estimate the global average of k, $\langle k \rangle$, over seven years
77 (1999-2006) using four k-U relationships. The objective of this paper is to compare these with
78 the new ^{14}C -derived k global averages, and to analyze to what extent the differences are
79 compatible with satellite wind speed uncertainty. With respect to previous $\langle k \rangle$ estimates
80 based on remotely sensed wind speeds, we use recent empirical k-U relationships and a longer
81 time series of wind speeds obtained with a single instrument (avoiding differences due to
82 instrument change) which allows us to estimate an interval of uncertainty for $\langle k \rangle$. The latter
83 is based on already published comparisons of QuikSCAT wind speeds with in situ wind
84 speeds and on new QuikSCAT / in situ wind speed comparisons in the northern Atlantic and
85 in the Southern Ocean. They cover a very large range of moderate to strong wind speeds,
86 enabling a validation of wind speed variability and intensity. This is all the more relevant for
87 air-sea CO_2 flux studies as the Southern Ocean is a region where very few wind validations
88 have been conducted, and where the CO_2 sink is quite large, because of strong wind speeds
89 [Boutin et al., 2002; Ho et al., 2006].

90 This paper is organized as follows: data and methods are described in section 2, the
91 uncertainty on QuikSCAT wind speeds is estimated in section 3, global averages of k are
92 presented in section 4, and the summary and conclusion are given in section 5.

93 **2 Data and Methods**

94 **2.1 Data**

95 **2.1.1 Satellite wind speeds**

96 Three types of satellite instruments have been used in the past to derive k from satellite wind
97 speeds (e.g., [Boutin and Etcheto, 1997; Carr et al., 2002]). The advantages and
98 disadvantages of each type of instrument for the determination of k as presented in previous
99 studies [Boutin and Etcheto, 1996, Boutin et al., 1999b] are summarized below.

100 An altimeter (e.g. Geosat, TOPEX-POSEIDON, JASON) measures the radar signal reflected
101 specularly to the instrument by the sea surface. It performs better at low to moderate wind
102 speeds. The altimeter wind speed is derived at about 7 km resolution. The altimeter swath is
103 narrow, about 5 km wide. Hence altimeter k fields are undersampled.

104 A microwave radiometer (e.g., SSMI, WindSat) measures the radiation emitted by the sea
105 surface at several wavelengths. Since the emissivity is dependent on geophysical parameters
106 (atmospheric water, SST, etc) other than surface wind, flaws in the correction of these effects
107 may lead to regional biases. Its swath is wide (1000-1400 km) and the resolution of individual
108 measurements is typically 25 km.

109 A scatterometer (e.g. ERS, NSCAT, QuikSCAT) measures the radar signal backscattered to
110 the instrument by the sea surface (Bragg scattering by gravity-capillary waves). It provides
111 very accurate satellite wind speed, in particular because it has very little sensitivity to
112 atmospheric conditions. Although wind speed retrieval from microwave radiometers such as
113 WINDSAT has improved, the scatterometer wind speeds have a better sensitivity at low and
114 moderate wind speeds [Quilfen et al., 2007]. Freilich and Vanhoff [2006], comparing satellite
115 with NDBC buoy wind speeds, found an rms difference of 1.2 m s^{-1} between QuikSCAT and
116 NDBC wind speeds and of 1.4 m s^{-1} between WINDSAT and NDBC wind speeds.
117 Scatterometer swaths are wide (500-1600km) and the resolution of individual measurements
118 varies between 12.5 and 50 km. Over a $1^\circ \times 1^\circ$ area and 10 days, there are approximately 240
119 independent wind speed measurements at 25km resolution derived from the QuikSCAT
120 scatterometer, whereas there are about 30 independent wind speed estimates from one
121 altimeter instrument.

122 In this study, we utilize QuikSCAT wind speeds from September 1999 to August 2006. In
123 order to take the effects of wind speed variability on k into account, we compute k for each
124 high resolution wind speed. We use the level 2B QuikSCAT wind speeds at 25 km resolution

125 derived at NASA/JPL (http://podaac.jpl.nasa.gov/DATA_PRODUCT/OVW/index.html;
126 nudge product processed with version 2.4 until May 2006; rain flagged wind speeds
127 discarded). A new version of QuikSCAT wind speeds was released in summer 2006. With
128 respect to version 2.4, high wind speeds (over 20 m s^{-1}) have been increased and flagging of
129 rain contamination has been improved. However, the comparison of weekly k fields generated
130 by the two versions for June 2006 shows small differences in large-scale k distributions: the
131 difference is lower than 2% in the global k average and lower than 3% in regional k averages.

132 **2.1.2 In situ wind speed**

133 QuikSCAT wind speeds are compared (1) in the northern Atlantic with wind speeds measured
134 during the POMME (Program Ocean Multidisciplinary MEscale) experiment on a
135 meteorological buoy and four CARIOCA drifters and (2) in the Southern Ocean with wind
136 speeds recorded on five CARIOCA drifters. Periods and locations of colocations are
137 summarized in Appendix A. In situ wind speeds are either measured at 2 m height, U2m, or at
138 4.5m height, U4.5m. They are adjusted to 10m height wind speed, U10m, either using a
139 constant drag coefficient, or using the *Liu and Tang* [1996] algorithm which computes the
140 wind speed at 10m height that would have been observed for the same friction velocity under
141 a neutrally stable atmosphere.

142 CARIOCA drifters are autonomous instruments primarily designed to measure parameters at
143 the air-sea interface related to air-sea CO₂ flux [*Bakker et al.*, 2001; *Hood and Merlivat*, 2001;
144 *Merlivat and Brault*, 1995]. They are designed for a period of autonomy of one year. In
145 addition to sea surface CO₂ partial pressure and fluorescence, they measure U2m, and (since
146 2004) air temperature at 2m height above the sea surface, the atmospheric surface pressure
147 and the sea surface temperature at 2m depth. CARIOCA drifters follow sea surface currents at
148 about 15m depth by using a “holey sock” drogue. Hence they measure the wind speed relative
149 to the sea surface drift (always less than 1 m s^{-1} ; averaged over all buoys in the Southern
150 Ocean, the east-west speed of the buoys is 0.2 m s^{-1}). Scatterometer measurements are
151 primarily sensitive to the surface wind stress and therefore to the wind speed relative to sea
152 surface currents [*Kelly et al.*, 2001; *Quilfen et al.*, 2001]. Consequently, the use of in situ wind
153 speeds relative to sea surface drift should reduce differences in the comparisons between in
154 situ and satellite wind speeds, avoiding regional biases due to the presence of strong currents.
155 In addition, k is also sensitive to surface wind stress so that wind speed relative to sea surface
156 drift and scatterometer wind speeds are better proxies for k than wind speed in a terrestrial
157 reference frame.

158 Before 2004, CARIOCA buoys were equipped with cup “Debucoart” anemometers.
159 Debucoart anemometers were tested during the TOSCANE-T campaign [*Queffeuou et al.*,
160 1988] on moored buoys. After two months, wind speeds measured by the three Debucoart
161 anemometers remained very consistent (mean bias negligible, equal to 0.03 m s^{-1} and the root
162 mean square of the differences equal to 0.18 m s^{-1}). Since 2004, CARIOCA buoys have been
163 equipped with Sonic CV3F anemometers built by the LCJ company
164 (<http://www.lcjcapteurs.com>). The sensitivity of the LCJ anemometer is 0.2m/s.

165

166 **2.1.2.1 Buoy wind speeds in the northern Atlantic Ocean**

167 The POMME experiment took place in 2000 and 2001 in the northeast Atlantic. Four
168 CARIOCA drifters were deployed and drifted between 36°N and 46°N and 12°W and 22°W .
169 The POMME meteorological buoy was moored at 20.04°W , 41.6°N and was equipped with a
170 cup anemometer from Vector instruments [*Caniaux et al.*, 2005] which recorded wind speed
171 at 4.5 m height above sea surface, U4.5m.

172 Both wind speeds are converted to 10m height wind speed, U10m, assuming a constant drag
173 coefficient, C_d , equal to 1.5×10^{-3} . This corresponds to an adjustment by a multiplicative
174 factor of 1.18 between U2m and U10m and 1.08 between U4.5m and U10m. Tests conducted
175 using the dependence of C_d on U measured during the POMME experiment show that the
176 approximation of a constant C_d does not significantly modify the two fits (mean U10m
177 modified by less than 1%). No correction for air stability was applied because air temperature
178 on CARIOCA buoys was not available before 2004, but an a posteriori correction will be
179 considered in section 3.4.

180

181 **2.1.2.2 In situ wind speeds in the Southern Ocean**

182 Between 2001 and mid-2006, nine CARIOCA drifters have been deployed in the Southern
183 Ocean. Unfortunately, some anemometers broke down very rapidly and problems with
184 onboard processing prevented wind speed measured by four of these drifters from being used.
185 Nevertheless, 5 CARIOCA drifters successively recorded wind speeds for 14 months between
186 40°S and 58°S , providing a unique set of wind speeds in this rough environment (see
187 Appendix A).

188 For conversion of U2m to neutral wind speeds at 10 m height, before 2004 the atmosphere is
189 assumed to be neutral. After 2004, air-sea temperature differences are taken into account.
190 Two-meter height wind speeds are converted to 10 m height neutral wind speeds, taking into
191 account air-sea temperature differences when available, using the *Liu and Tang* [1996]

192 algorithm typically used to validate scatterometer wind speeds with in situ measurements, and
193 assuming a relative humidity of 80%. For a neutral atmosphere, the conversion factor is
194 minimum at 5 m s^{-1} (1.16) and increases at lower and higher wind speeds (1.2 at 15 m s^{-1}).
195 The influence of atmospheric stability is small at high wind speed. However, in the Southern
196 Ocean the atmosphere is frequently colder than the surface ocean by several degrees so that
197 not correcting for atmospheric stability may lead to a small bias in 10m neutral wind speed
198 estimates. From 2006 CARIOCA data, we find that the atmosphere stability correction
199 increases the mean CARIOCA 10m wind speed by 0.15 m s^{-1} .

200 **2.1.3 Sea surface temperature**

201 The sea surface temperature, SST, is taken from monthly SST maps derived using a blended
202 analysis between AVHRR (Advanced Very High Resolution Radiometer) and in situ data
203 according to the method described in *Reynolds et al.* [2002]. These maps are available at
204 ftp://podaac.jpl.nasa.gov/pub/sea_surface_temperature/reynolds/oisst/data/oiweek_v2.

206 **2.2 Methods**

207 **2.2.1 k computation**

208 When dealing with the relationship between k and sea state and gas parameters, experimental
209 k is usually expressed at a constant Schmidt number of 600 (corresponding to the CO_2
210 Schmidt number in fresh water at a temperature of 20°C , e.g., [*Nightingale et al.*, 2000] and
211 [*Ho et al.*, 2006]) or 660 (corresponding to the CO_2 Schmidt number in sea water at a
212 temperature of 20°C , e.g., [*Wanninkhof*, 1992]). When studying air-sea CO_2 flux over the
213 ocean it is necessary to take temperature variation into account, since k varies by more than a
214 factor of 2 between 0° and 30°C for CO_2 gas due to variation of the Schmidt number with
215 temperature. This is the reason why, when treating air-sea CO_2 flux using bulk formula
216 (equation (1)), it is more convenient to consider the CO_2 exchange coefficient, $K=k S$, as
217 temperature variations of k and S almost compensate for each other [*Etcheto and Merlivat*,
218 1988]. Taking the variation of K as proportional to $((S_c/660)^{-0.5} S)$, K varies by less than 10%
219 between 0 and 30°C . In this paper, we derive a global mean value of k , $\langle k \rangle$, from $\langle K \rangle$, the
220 global mean value of K , using a constant ratio between $\langle k \rangle$ and $\langle K \rangle$ defined below. The K
221 fields are derived from high resolution wind speed data and sea surface temperature maps as

222 described in Appendix B. The temporal and spatial variability of K from 1999 to 2006 is
223 presented in Appendix B.

224 The following k-U relationships are considered in this paper:

225 -The *Liss and Merlivat* [1986] relationship, which takes into account the physics of the air-sea
226 interface, deduced from wind tunnel measurements, and from lake measurements for
227 normalization. It is divided into three regimes: smooth surface, rough surface and breaking
228 waves regimes:

$$229 \quad k_{LM}=0.17 U (600/Sc)^{2/3} \quad \text{for} \quad U \leq 3.6 \text{ m s}^{-1} \quad (2.1)$$

$$230 \quad k_{LM}=(2.85 U - 9.65) (600/Sc)^{0.5} \quad \text{for} \quad 3.6 \text{ m s}^{-1} < U \leq 13 \text{ m s}^{-1} \quad (2.2)$$

$$231 \quad k_{LM}=(5.9 U - 49.3) (600/Sc)^{0.5} \quad \text{for} \quad U > 13 \text{ m s}^{-1} \quad (2.3)$$

232 -The *Wanninkhof* [1992] quadratic relationship deduced from a quadratic fit to the GEOSECS
233 bomb ^{14}C inventory for short term wind speed:

$$234 \quad k_W = 0.31 U^2 (660/Sc)^{0.5} \quad (3)$$

235 -The *Nightingale et al.* [2000] relationship deduced from dual tracer experiments at sea:

$$236 \quad k_N = (0.222 U^2 + 0.333 U) (600/Sc)^{0.5} \quad (4)$$

237 - The *Ho et al.* [2006] relationship recently derived from k measurements performed during
238 the SAGE experiment in the Southern Ocean. It is a quadratic k-U relationship close to the
239 second order polynomial relationship of *Nightingale et al.* [2000] and 22% lower than that of
240 *Wanninkhof* [1992]. The k corresponding to the *Ho et al.* [2006] relationship ($k_H=0.266 U^2$
241 $(600/Sc)^{0.5}$) is deduced from k_W as:

$$242 \quad k_H=0.818 k_W \quad (5)$$

243 Recently, *Sweeney et al.* [2007] proposed a new relationship based on a new analysis of ^{14}C
244 measurements ($k=0.27 U^2 (660/Sc)^{0.5}$) that are equal to $0.87 \times k_W$.

245 These k-U relationships, for a Schmidt number of 660 are shown in Appendix B.

246 A cubic k-U relationship is not considered, as results from the SAGE (SOLAS Air-Sea Gas
247 Exchange) experiment reveal that a quadratic k-U relationship is closer to the measurements
248 than a cubic relationship [*Ho et al.*, 2006], and because differences between quadratic and
249 cubic relationships have already been studied [*Boutin et al.*, 2002].

250 We compute k from high resolution wind speed in order to take correctly into account the
251 wind speed variability in the non-linear k-U relationship. Actually, *Wanninkhof et al.* [2002]
252 show that, on a local scale, the statistical distribution of wind speed frequently differs from a
253 Rayleigh distribution so that relationships between k and "long-term" (averaged) wind speeds
254 calibrated assuming a Rayleigh distribution such as the one proposed by *Wanninkhof* [1992]
255 overestimate k [*Olsen et al.*, 2005].

256 The global k averages presented in the following sections are deduced from the temporal and
 257 spatial integration (area weighted) of K fields. Deriving a global average of k, either from the
 258 global average of K or from the global average of k at a Schmidt number of 660, $\langle k_{660} \rangle$, as
 259 reported by some authors, is not straightforward because, over the global ocean, wind speed
 260 and sea surface temperature are anticorrelated. In order to find conversion factors between
 261 $\langle k \rangle$, $\langle K \rangle$ and $\langle k_{660} \rangle$, we compute their ratios over one year (2003) as derived from
 262 QuikSCAT wind speeds and for a quadratic k-U relationship:

$$263 \quad \langle K[\text{mol/m}^2/\text{yr}/\mu\text{atm}] \rangle / \langle k[\text{cm/hr}] \rangle = 3.25 \times 10^{-3} \quad (6)$$

$$264 \quad \langle k \rangle / \langle k_{660} \rangle = 0.93 \quad (7)$$

265 These ratios vary by less than 1% from one year to another.

266 The mean difference between $\langle k \rangle$ and $\langle k_{660} \rangle$ is mainly because the global average of SST is
 267 closer to 18°C than to 20°C and because of wind speed-sea surface temperature
 268 anticorrelation; it is consistent with the 6% bias found by *Sweeney et al.* [2007] on the
 269 calibration of the *Wanninkhof* [1992] k-U relationship which was performed using a constant
 270 solubility at 20°C.

271

272 **2.2.2 Colocation of QuikSCAT with in situ wind speed**

273 Each in-situ wind speed is collocated with QuikSCAT measurements taken within a radius of
 274 12.5km and 30 min. Fits between in situ and QuikSCAT wind speeds are calculated as
 275 orthogonal regressions, which makes the implicit assumption that the noise on in situ and
 276 QuikSCAT wind speeds is similar. The fit quality is quantified by the 95% confidence
 277 interval of the fit slope and by the rms (root mean square) of QuikSCAT wind speed minus
 278 the fit estimate (rms of (Y-Yfit)).

279 CARIOCA wind speeds are measured every hour but each measurement is integrated over a
 280 very short duration (30s) in order to save energy. Hence, before comparing QuikSCAT and
 281 CARIOCA wind speeds, CARIOCA wind speeds are smoothed with a running average over 3
 282 consecutive measurements weighted by (0.25, 0.5, 0.25) factors. Assuming a rough
 283 equivalence between time and space integration that follows the hypothesis of frozen
 284 turbulence ($\Delta S = U \Delta T$, where ΔS is the spatial extent of the integration, ΔT is the integration
 285 duration and U is the wind speed), an integration over 25km, close to QuikSCAT wind speed
 286 resolution, is roughly equivalent to an integration over 2 hours at 10m/s. This is consistent
 287 with a running average over 3 consecutive buoy measurements. This running average
 288 decreases the rms of (Y-Yfit) by about 20% without significant change in the orthogonal fit.

289 Without this running average, the standard deviation of CARIOCA wind speeds is increased
290 by about 4% and estimates of the mean of U squared do not significantly change.

291

292 **3 QuikSCAT wind speed uncertainty**

293 The validation of satellite wind speed is a tricky task as (1) calibration of in situ wind speed
294 measurements within a few tenths of m s^{-1} is difficult, (2) wind speed is very variable inside a
295 satellite pixel (25km resolution), and (3) the parameters necessary to compute neutral
296 equivalent wind speed at 10m height, (wind speed, relative humidity and air temperature at
297 10m height, sea surface temperature and currents) are rarely available.

298 In this section, after recalling recent results for QuikSCAT validation, we present a new set of
299 comparisons between QuikSCAT and in situ wind speeds in the Northern Atlantic at more
300 than 350km from coasts and in the Southern Ocean at more than 500km from continental
301 coasts. This is intended to evaluate QuikSCAT wind speed over a large range of moderate to
302 high wind speeds, in regions not frequently sampled by buoys typically used for QuikSCAT
303 validation.

304

305 **3.1 Previous studies**

306 Several studies have inferred the quality of QuikSCAT wind speeds from comparison with
307 either buoys, ship or model wind speeds. Comparisons with in situ data [*Bourassa et al.*,
308 2003; *Ebuchi et al.*, 2002; *Freilich and Vanhoff*, 2006] indicate a root mean square accuracy
309 of QuikSCAT wind speeds between 1 and 1.2m s^{-1} in conditions without rain. There was no
310 evidence for large systematic biases in QuikSCAT wind speeds. *Ebuchi et al.* [2002]
311 compared QuikSCAT with wind speeds of buoys operated by the National Data Buoy Center
312 (NDBC), Tropical Atmosphere Ocean (TAO), Pilot Research Moored Array in the Tropical
313 Atlantic (PIRATA) project and Japan Meteorological Agency (JMA) in the tropical oceans
314 and in the northern hemisphere,. They found no systematic dependence of buoy-QuikSCAT
315 wind residuals between 5 and 15 m s^{-1} and mean residuals of about -0.5 m s^{-1} for wind speeds
316 greater than 15 m s^{-1} but these latter results have to be taken with caution given the difficulty
317 of measuring high in situ wind speeds. *Freilich and Vanhoff* [2006] found that there were
318 relatively slightly more QuikSCAT wind speeds in the band $10\text{-}16\text{ m s}^{-1}$ than NCEP (U.S.
319 National Centers for Environmental Prediction operational numerical weather prediction
320 model) wind speeds when looking at the statistical distributions of colocated wind speeds. It

321 is unlikely that the latter is only due to a larger smoothing of wind speed variability by NCEP
 322 than by QuikSCAT as *Freilich and Vanhoff* [2006] observed similar differences in the
 323 statistical distributions of QuikSCAT wind speeds colocated with NDBC (National Data
 324 Buoy Center) buoy wind speeds. These slight differences in wind speed distributions did not
 325 affect the average of colocated wind speed because they were compensated by slightly lower
 326 QuikSCAT than NCEP wind speeds between 5 and 8m s⁻¹. The mean QuikSCAT wind speed,
 327 $\langle U_{qscat} \rangle$, is 7.23 m s⁻¹ and the mean NCEP wind speed, $\langle U_{ncep} \rangle$, is 7.22 m s⁻¹. On the other
 328 hand, the differences in wind speed distributions affect the standard deviation: the standard
 329 deviation of QuikSCAT wind speeds, σ_{qscat} , equals 3.04 m s⁻¹, while the standard deviation
 330 of NCEP wind speeds, σ_{ncep} , equals 2.68 m s⁻¹. Assuming that k is proportional to the square
 331 of U, we can compute the ratio between the mean of k derived from QuikSCAT wind speeds,
 332 $\langle k_{qscat} \rangle$ and the mean of k derived from NCEP wind speeds, $\langle k_{ncep} \rangle$ as:

$$334 \frac{\langle k_{qscat} \rangle}{\langle k_{ncep} \rangle} = \frac{\langle U_{qscat} \rangle^2 + \sigma_{qscat}^2}{\langle U_{ncep} \rangle^2 + \sigma_{ncep}^2} \quad (8)$$

335 We find a 1.04 ratio between $\langle k_{qscat} \rangle$ and $\langle k_{ncep} \rangle$. Over the global ocean, the difference
 336 may be even larger as the colocated distributions studied by *Freilich and Vanhoff* [2006] were
 337 limited to low and middle latitudes and hence were biased towards low to moderate wind
 338 speed. Up to the present date most of the QuikSCAT-in situ wind speeds comparisons were
 339 based on measurements taken in the equatorial region and in the northern hemisphere.

340 **3.2 Comparison of QuikSCAT with in situ wind speed in the** 341 **northern Atlantic**

342 The scatter plot of the comparisons between QuikSCAT and CARIOCA wind speeds is
 343 shown on Figure 2, top and the statistics are given in Table 1. The scatter of the points is
 344 remarkably low, the rms of QuikSCAT wind speed with respect to the orthogonal fit being
 345 always lower than 1.03m s⁻¹. This illustrates the excellent sensitivity of the scatterometer
 346 signal to wind speed.

347 Buoy 10m wind speeds are systematically lower than QuikSCAT by 13% for CARIOCA and
 348 4% for the moored buoy (Table 1). The comparison of the two fits indicates that for
 349 QuikSCAT wind speeds equal to 10m s⁻¹, CARIOCA wind speeds are lower than moored
 350 buoy wind speeds by about 8%. Both fits have a slope significantly higher than 1.

351 **3.3 Comparison of QuikSCAT with in situ wind speed in the**
352 **Southern Ocean**

353 The scatter plot of the comparisons between QuikSCAT and CARIOCA wind speeds is
354 shown on Figure 2, bottom and the statistics are given in Table 1. The scatter of the points is
355 as low as in the northern Atlantic, about 1 m s^{-1} , confirming the excellent correlation of
356 QuikSCAT wind speeds with in situ wind speeds. The orthogonal fit found between the
357 CARIOCA wind speeds as measured with the Debucoart anemometer and QuikSCAT wind
358 speeds is very similar to that found over the POMME area. Both fits have a slope significantly
359 higher than 1. For the same QuikSCAT wind speed values, sonic anemometer wind speeds are
360 about 1 m s^{-1} higher than Debucoart anemometer wind speeds.

361 **3.4 Discussion**

362 **3.4.1 In situ wind speed**

363 The fits between QuikSCAT and CARIOCA wind speeds measured with the Debucoart
364 anemometer in the northern Atlantic and in the Southern Ocean are very similar, indicating a
365 similar bias of QuikSCAT wind speeds in the Southern Ocean and in the northern Atlantic
366 Ocean even though sea state conditions may be different. In both cases, the ratio between
367 QuikSCAT and CARIOCA-Debucoart wind speeds computed from mean values reported in
368 Table 1 is 1.16. However, the fits between QuikSCAT and meteorological buoy wind speeds
369 in the northern Atlantic Ocean and between QuikSCAT and CARIOCA sonic wind speeds in
370 the Southern Ocean are both lower (by 0.8 m s^{-1} for a QuikSCAT wind speed of 10 m s^{-1}) than
371 the values given by the fits between QuikSCAT and CARIOCA-Debucoart anemometer wind
372 speeds. Hence an underestimation of 8% for CARIOCA-Debucoart wind speeds cannot be
373 excluded. Once this effect is accounted for, and once a correction of 0.15 m s^{-1} for neutral
374 atmosphere assumption (see section 2.1.2.2) is added to our comparisons, CARIOCA wind
375 speeds in the northern Atlantic Ocean and in the Southern Ocean still remain lower than
376 QuikSCAT wind speeds by about 5% (Table 2). In addition the variability of in situ wind
377 speed is found to be lower than the variability of QuikSCAT wind speeds. Using an equation
378 similar to equation (8), we find ratios of 1.08 to 1.12 between mean k deduced from
379 QuikSCAT wind speeds and from in situ wind speeds (Table 2, last column).

380 Since this difference is estimated from 9 buoys of 3 different types, in several oceans and at
381 various seasons, it is unlikely that it is due to a flaw in anemometer calibration. One
382 uncertainty could result from the model that we use to convert 2m height wind speed to 10m

383 height neutral wind speed. The wind stress drag coefficients C_d , deduced from the *Liu and*
384 *Tang* [1996] algorithm, vary between 1.1×10^{-3} at 5m s^{-1} and 1.7×10^{-3} at 15m s^{-1} . These
385 values agree well with the parametrization of C_d deduced from measurements performed in
386 the northern Atlantic during the POMME experiment [*Caniaux et al.*, 2005]. In order to
387 increase the conversion factor between $U_{2\text{m}}$ and $U_{10\text{m}}$ by 5%, C_d at 15m/s should reach 2.5
388 $\times 10^{-3}$. Although large uncertainties remain in C_d because it depends on parameters other than
389 wind speeds, this value appears larger than C_d estimated using wave-age or wave-steepness
390 formula in wind sea conditions at high wind speed (Figure 9a of *Drennan et al.* [2005]
391 showing C_d close to 2×10^{-3} at 15m s^{-1} in wind sea conditions) and over the global ocean by
392 *Kara et al.* [2007].

393 **3.4.2 QuikSCAT wind speed uncertainty:**

394 Once possible biases in in situ wind speeds have been corrected (about 0.7m s^{-1} at 14m s^{-1}),
395 the buoy-QuikSCAT wind speed differences we observe are slightly higher than those shown
396 in *Ebuchi et al.* [2002]. Like [*Freilich and Vanhoff*, 2006], we find greater variability in
397 QuikSCAT wind speed than in in situ wind speed; however the ratio between averages of U
398 squared is slightly higher in our study (Table 2, last column) than are those deduced from
399 their study (see section 3.1). Measuring in situ neutral wind speed with an absolute accuracy
400 better than 0.5m s^{-1} is very challenging and we cannot definitely assert that our in situ wind
401 speeds are free of biases. On the other hand, validation of QuikSCAT wind speed is also very
402 challenging because few high wind speeds are measured in situ onboard NDBC and tropical
403 buoys, while Ku band scatterometer measurements saturate at high wind speed and rain
404 disturbs wind speed retrieval. In this paper we have presented a new set of in situ
405 measurements allowing the validation of QuikSCAT wind speeds in regions that have never
406 been validated from buoy observations in the past (Southern Ocean) and where high wind
407 speeds occur.

408 All these studies agree on the fact that scatterometer QuikSCAT wind speeds are of extremely
409 good quality, but that, in the worst case scenario, they could suffer from an overestimation by
410 less than 5%. Hence, in the following analyses, we assume that QuikSCAT wind speed can be
411 taken as the reference wind speed, but we have also performed a sensitivity study in which
412 QuikSCAT wind speeds are diminished by 5%, as a lower bound for the absolute accuracy of
413 QuikSCAT wind speed.

414

415 **4 Global k average**

416 **4.1 QuikSCAT estimate**

417 Averaged over seven years, $\langle k_w \rangle$ and $\langle k_{LM} \rangle$ deduced from QuikSCAT wind speeds (21.1
418 and 11.9 cm hr⁻¹, respectively; Figure 1), differ by a ratio of 1.8. With respect to previous
419 studies using older satellite wind speeds, they are higher by about 17% (Figure 1). When
420 QuikSCAT wind speeds are lowered by 5%, $\langle k \rangle$ is lowered by 10% for a quadratic k-U
421 relationship. Hence, the difference from previous satellite estimates becomes close to 6%
422 (Figure 1). Nevertheless this difference remains larger than the interannual variability of k
423 (see Figure 3 and Appendix B) and may be due to inaccuracies in previous satellite wind
424 speeds. Indeed, *Boutin et al.* [1999b] show that the global k derived from ERS2 and NSCAT
425 wind speeds differs by about 8%, partly because of ERS2 wind speed underestimation.

426 The $\langle k_H \rangle$ (17.3 cm hr⁻¹) and $\langle k_N \rangle$ (17.5cm hr⁻¹) differ by only 0.2cm hr⁻¹ (1.2%) which is
427 lower than the k-U relationships error estimate: *Ho et al.* [2006] estimate a precision of 0.019
428 (7%) in the coefficient of their quadratic relationship, which leads to a precision of 1.2 cm hr⁻¹
429 ¹ in the k global average. The $\langle k_N \rangle$ value is slightly higher than $\langle k_H \rangle$ although k_H is higher
430 than k_N above 9m s⁻¹, showing the importance of low to moderate wind speeds for the global
431 k average, as already observed by *Boutin et al.* [2002]. The $\langle k_w \rangle$ differs from $\langle k_H \rangle$ and $\langle k_N \rangle$
432 by a ratio of 1.22 and 1.20 respectively.

433 **4.2 Comparison with ¹⁴C and various satellite estimates of k**

434 The $\langle k \rangle$ values deduced from the new ¹⁴C constraints, corrected with equation (7) when
435 necessary, are reported on Figure 1. The three mean values estimated using the GEOSECS
436 and the recent WOCE inventories by [*Krakauer et al.*, 2006; *Naegler et al.*, 2006; *Sweeney et*
437 *al.*, 2007] are consistent (within the error bars of each estimate). Nevertheless, we attach less
438 confidence to the value reported by *Krakauer et al.* [2006], because it implies a linear
439 dependency of k with wind speed, which is not observed in field data.

440 The $\langle k \rangle$ values obtained with the *Liss and Merlivat* [1986] relationship and QuikSCAT wind
441 speeds do not satisfy the new ¹⁴C constraints proposed by *Krakauer et al.* [2006] and by
442 *Naegler et al.* [2006] (Figure 1) and are in the lower bound of the estimate in *Sweeney et al.*
443 [2007]. The $\langle k_H \rangle$ and $\langle k_N \rangle$ are in the upper part of the $\langle k \rangle$ estimates proposed by *Naegler et*
444 *al.* [2006] and *Sweeney et al.* [2007]. Closer agreement is found with the new ¹⁴C constraints
445 proposed by *Naegler et al.* [2006] and *Sweeney et al.* [2007] with k_N derived from QuikSCAT
446 wind speeds lowered by 5%. The 5% correction is not applied to k_H as the relationship

447 presented in [Ho *et al.*, 2006] was deduced from QuikSCAT wind speeds. The $\langle k_w \rangle$ value
448 derived from QuikSCAT wind speeds does not satisfy the new ^{14}C constraint of Naegler *et al.*
449 [2006] and Sweeney *et al.* [2007]. When QuikSCAT wind speeds are lowered by 5%, $\langle k_w \rangle$ is
450 in the upper error bar of these new ^{14}C estimates, but it remains 2.4 to 4.4 cm hr $^{-1}$ higher than
451 their averages.

452 It is interesting to compare $\langle k \rangle$ derived in this study with the one derived by Frew *et al.*
453 [2007]. They used an empirical relationship between k and mean-square slope (mss) based on
454 field measurements and mss derived from dual frequency altimeter data, using a simple
455 geometric optics model. They found a global mean k equal to 13.7 ± 4.1 cm hr $^{-1}$, lower but
456 consistent with our estimate of $\langle k_N \rangle$ and $\langle k_H \rangle$. Their mean estimate is closer to $\langle k_N \rangle$ after
457 correcting QuikSCAT wind speed by 5%. This is consistent with the fact that the estimations
458 of k during the CoOP97 campaign, used to calibrate k -mss relationship, were close to the
459 [Nightingale *et al.*, 2000] k -U dependency (Figure 4 of Frew *et al.* [2004]).

460 **4.3 Consequences on air-sea CO $_2$ flux**

461 Air-sea CO $_2$ fluxes are derived using equation (1) and $\Delta p\text{CO}_2$ fields taken from the Takahashi
462 *et al.* [2002] climatology. They are reported in Table 3 together with fluxes available at
463 http://www.ldeo.columbia.edu/res/pi/CO2/carbondioxide/text/10m_wind.prn which were
464 derived from the same $\Delta p\text{CO}_2$ fields, the NCAR/NCEP 41-Year Reanalysis Wind Data at
465 10m height, and the long-term Wanninkhof (1992) k -U relationship. The global flux we
466 deduce from k_w and [Takahashi *et al.*, 2002] $\Delta p\text{CO}_2$ fields is 8% more negative than that
467 derived from 41 years of NCAR/NCEP reanalyzed wind speeds and the Wanninkhof long-
468 term relationship (-1.64 PgC yr $^{-1}$). As shown by Olsen *et al.* [2005], this is mainly because of
469 differences between NCAR/NCEP reanalysis wind speeds and QuikSCAT wind speeds. This
470 is also partly consistent with the different variability between NCEP and QuikSCAT wind
471 speed as seen by Freilich and Vanhoff [2006], which leads to a 4% difference in term of k
472 (see section 3.1). All the fluxes indicated in Table 3 correspond to original QuikSCAT wind
473 speeds. If QuikSCAT wind speeds are decreased by 5%, the absolute value of the fluxes
474 would be decreased by 10% for quadratic relationships. With respect to the regional fluxes
475 listed in Table 3, the greatest effect would be observed in the largest sink regions, between
476 14°S and 50°S.

477 The global yearly air-sea CO $_2$ fluxes which we derive using k_w vary between -1.71 PgC yr $^{-1}$
478 and -1.83 PgC yr $^{-1}$ (7 years mean equal to -1.77 PgC yr $^{-1}$). These values are close to the 2000-
479 2003 air-sea CO $_2$ fluxes derived by Olsen *et al.* [2005] using the same k -U relationship and

480 QuikSCAT wind speeds (4 year mean equal to -1.73PgC yr^{-1}). The variability of the fluxes in
481 latitude obtained with k_w has already been discussed in previous studies (e.g [Boutin *et al.*,
482 2002], [Olsen *et al.*, 2005]). In what follows, we concentrate on the differences linked to the
483 use of different k - U relationships.

484 If k_H , k_N or k_{LM} are used to compute the fluxes instead of k_w , the mean global absorbing flux
485 is reduced to 1.45, 1.39 and 0.93PgC yr^{-1} , respectively. The main differences in the regional
486 fluxes are observed in regions where the fluxes are the greatest because of their large surface
487 areas and/or because of the large disequilibrium between atmospheric and oceanic pCO_2 , in
488 the tropical band (decrease of the outgassing flux by 0.19PgC yr^{-1} with k_H instead of k_w) and
489 in the subtropics (decrease of the downward flux in the bands 14°N - 50°N and 14°S - 50°S by
490 0.37PgC yr^{-1} when using k_H instead of k_w). Fluxes obtained with k_H and k_N are very similar
491 except in the equatorial band because k_H is lower than k_N at low wind speed.

492 The mean global absorbing fluxes deduced from k_H and k_N are 1.45 and 1.39PgC yr^{-1}
493 respectively. However, uncertainty remains in these estimates: given the absolute accuracy in
494 QuikSCAT wind speed and in the new ^{14}C constraint, the flux may be overestimated by 10%
495 at most. In addition, ΔpCO_2 fields are going to be reduced in future estimates as *Takahashi et*
496 *al.* [2002] did not correct ocean pCO_2 measurements for the atmospheric trend in some
497 regions, although recent studies have shown that a correction should be applied [*Feely et al.*,
498 2006; *Rangama et al.*, 2005]. This correction should lead to a significant decrease in
499 absorbing air-sea CO_2 flux. (See Takahashi, July 2006, presentation at Woods Hole, available
500 at <http://www.us-ocb.org/meetings/2006/agenda.html>).

501

502 **5 Summary and conclusions**

503 The quality of satellite wind speeds has greatly improved over the last two decades, and today
504 estimates of the root mean squared accuracies of scatterometer wind speeds are around 1m s^{-1} .
505 This makes it possible to monitor wind speed variability very well. Nevertheless, when
506 dealing with parameters proportional to the square of U , such as k , the absolute accuracy
507 requirement for both mean and standard deviation of wind speed is very stringent. Given
508 previous QuikSCAT wind speed validation studies and the new comparisons shown in this
509 paper, we conclude that the QuikSCAT operational products are accurate to 5% or better. The
510 new comparisons demonstrate the difficulty of assessing the absolute accuracy of satellite
511 wind speeds over the global ocean, given the difficulty of acquiring high-quality estimates of
512 neutral equivalent wind speed over various regions of the open ocean and they provide

513 QuikSCAT-buoy wind speed comparisons in the Southern Ocean for the first time. Buoy
514 wind speed data used for satellite wind speed validation have typically been acquired at a
515 height lower than 10m, in non-neutral conditions and in the tropics or in the northern
516 hemisphere. In our $\langle k \rangle$ determinations, QuikSCAT operational products are used as the
517 reference wind speed; however, given the results of our new comparisons, we have also
518 performed a sensitivity study in which QuikSCAT wind speeds are diminished by 5%,
519 making the implicit assumption that the actual neutral wind speed is bounded between the
520 QuikSCAT value and the QuikSCAT value minus 5%.

521 The $\langle k_H \rangle$ and $\langle k_N \rangle$ differ by 1.5% when QuikSCAT wind speeds are used for their
522 computation. The polynomial function used by *Nightingale et al.* [2000] was chosen because
523 the *Liss and Merlivat* [1986] relationship, which is physically based, fitted better with a
524 second-order polynomial function than with a quadratic function. However, the differences
525 we observe are within the precision of these relationships. The $\langle k_{LM} \rangle$ and $\langle k_W \rangle$ are quite far
526 from new ^{14}C derived $\langle k \rangle$ although, given the uncertainty of QuikSCAT wind speeds and on
527 ^{14}C k estimates, they remain at the very lower and very upper bounds of the error intervals
528 (Figure 1). On the other hand, the $\langle k_H \rangle$ and $\langle k_N \rangle$ are fully consistent with new ^{14}C
529 constraints. Hence, the introduction of an “inventory normalized gas exchange parameter”
530 intended to adjust $\langle k \rangle$ to ^{14}C constraint for a given wind field, as proposed by *Naegler et al.*
531 [2006], is not relevant when using high resolution QuikSCAT wind speed. Indeed, the
532 difference between QuikSCAT $\langle k \rangle$ and ^{14}C constraint may either be due to a bias in
533 QuikSCAT wind speeds or to uncertainties in ^{14}C values. On the other hand, if QuikSCAT
534 wind speeds are overestimated by 5%, the coefficient of the k-U relationships determined by
535 *Ho et al.* [2006] should be increased by 10% (as the relationship was derived using
536 QuikSCAT wind speeds).

537 Taking into account wind speed uncertainty, the global mean of air-sea CO_2 fluxes derived
538 with the transfer velocities that are in close agreement with new ^{14}C constraints (k_H and k_N)
539 and with $\Delta p\text{CO}_2$ fields taken from *Takahashi et al.* [2002] climatology, is between -1.36 and
540 -1.45PgC yr^{-1} . Although the calibration of k-U relationships has been greatly advanced by the
541 new ^{14}C inventories, new experiments are still needed (1) to analyze the impact of sea surface
542 parameters other than U on k, (2) to study the impact of such alternative parametrizations on
543 global k fields with respect to k-scatterometer U fields and (3) to improve the k-U
544 relationships by additional in situ flux measurements. It is critical to measure wind speeds
545 very accurately, as a 5% bias in U leads to a 10% bias in k.

546

547 **Appendix A: In situ wind speed colocated with QuikSCAT wind speeds**

548 Periods and locations of QuikSCAT-in situ wind speeds colocations are summarized in Table
549 A 1. In the northern Atlantic, CARIOCA drifters were deployed and drifted between 36°N
550 and 46°N and 12°W and 22°W; trajectories are presented in [Merlivat *et al.*, 2008]. In the
551 Southern Ocean, they drifted in the southern Atlantic ocean and in the Indian Ocean as shown
552 in Figure A 1.

553

554 **Appendix B: Air-sea CO₂ exchange coefficients**

555 For each 25km resolution QuikSCAT wind speed, k is computed using relationships (2)
556 through (5). These relationships are restated in Figure B 1.

557 The temperature-Schmidt number dependency is taken from [Wanninkhof, 1992]. An estimate
558 of K is obtained by multiplying k by the solubility derived using the temperature-solubility
559 dependence given by Weiss [1974]. K deduced with the k - U relationships of Liss and
560 Merlivat [1986], Wanninkhof [1992], Nightingale *et al.* [2000] and Ho *et al.* [2006] are
561 named K_{LM} , K_W , K_N and K_H respectively.

562 Weekly and monthly 1°x1° resolution K maps are obtained by interpolating K using the
563 IFREMER kriging method described in [Bentamy *et al.*, 1996]. This method was validated by
564 the comparison of satellite interpolated wind speeds with in situ wind speeds and it is
565 routinely used at CERSAT/IFREMER for wind speed interpolations [Bentamy and J.F.Piollé,
566 2002]. In order to ensure consistency with previous K fields derived using a simpler objective
567 analysis method [Boutin and Etcheto, 1997], at LODYC (Laboratoire d'Océanographie
568 Dynamique et de Climatologie), K maps obtained with the two methods were compared.

569 The K global average deduced from QuikSCAT wind speeds with the IFREMER
570 interpolation method over 5 years is only 0.7% higher than the K global average deduced
571 from the LODYC method. This result was obtained with the non linear [Liss and Merlivat,
572 1986] and the [Wanninkhof, 1992] quadratic relationships. The standard deviation of the
573 differences between LODYC and IFREMER K_{LM} interpolated on weekly fields at 1°x1°
574 resolution is $0.38 \times 10^{-2} \text{ mol m}^{-2} \text{ yr}^{-1} \mu\text{atm}^{-1}$, i.e. 10% of the global K average. This is mainly
575 because the LODYC method smoothes more small scale spatial variations than the IFREMER
576 method.

577 Monthly zonal averages of K derived with the [Wanninkhof, 1992] k - U relationship are
578 presented in Figure B 2. This k - U relationship was chosen because it is the most widely used
579 in the scientific community. The figure results can be converted to other quadratic k - U

580 relationships ($k=aU^2 (660/Sc)^{0.5}$) by multiplying the color scale by $a/0.31$. So, for the *Ho et al.*
581 [2006] relationship, the scale has to be multiplied by 0.818 and ranges from 0.017 to 0.15 mol
582 $m^{-2} yr^{-1} \mu atm^{-1}$.

583 Monthly zonal averages of K follow the classical latitudinal and seasonal variations [*Boutin*
584 *and Etcheto*, 1997]: minimum of K in the tropics, maximum at high latitudes with a seasonal
585 cycle much weaker in the Southern Ocean than at high northern latitudes, K stronger in the
586 southern Indian Ocean than in the southern Pacific and Atlantic Ocean. In addition, monthly
587 K averaged over all longitudes exhibits interannual variability, e.g. a decrease of K in the
588 Southern Ocean during the austral winter 2002 due to K decrease in the southern Pacific
589 Ocean, a decrease of K in boreal winters 2003-2004 and 2005-2006 in the high northern
590 latitudes due to K decrease in the Atlantic Ocean, and an increase of K at the end of 2003 in
591 the southern tropics.

592 The mean monthly K values obtained with the four k-U relationships in five latitudinal bands
593 and over the global ocean are shown in Figure B 3. For all latitudinal band, K_{LM} is lower than
594 K_N which in turn is lower than K_W . The ratios between the various K are variable depending
595 on the wind speed distribution in the latitudinal band, as already discussed in *Boutin et al.*
596 [2002]. K_N and K_H are very close to each other as is to be expected from the k-U relationships
597 (see Figure A 1): both k-U relationships give the same k at $7.6m s^{-1}$. For lower U, k_N is
598 slightly higher than k_H (a difference of less than $1cm hr^{-1}$) and for higher U, k_N is lower than
599 k_H . The difference remains less than 10% for U up to $16m s^{-1}$. These small differences lead to
600 a peak-to-peak seasonal variation of K that is about 5% higher for K_H than for K_N in the high
601 northern latitudes (Figure B 3, top left). When averaged over the global ocean, K exhibits no
602 seasonal variation. Mean global values (and the standard deviation of monthly mean global
603 values from September 1999 to August 2006) of K_W , K_H , K_N and K_{LM} are $6.86 (\pm 0.18)$, 5.61
604 (± 0.15) , $5.69 (\pm 0.14)$, and $3.88 (\pm 0.10) \times 10^{-2} mol m^{-2} yr^{-1} \mu atm^{-1}$ respectively.

605 Using the conversion factors given in section 2.2.1, the color scale of Figure B 2 corresponds
606 approximately to k_H at a Schmidt number of 660 varying from $5cm hr^{-1}$ to $46cm hr^{-1}$. The
607 seasonal and interannual variability seen on monthly zonal k distributions derived from our
608 Figure B 2 are very similar to the ones derived from the altimetric mss and k-mss relationship
609 by [*Glover et al.*, 2007] as shown on their Figure 4. In particular, both studies show a
610 decrease of k in the Southern Ocean during the austral winter 2002, a decrease of k in the
611 boreal winter 2003-2004 in the high northern latitudes and an increase of k at the end of 2003
612 in the southern tropics.

613

614 *Acknowledgments :*

615 We thank three anonymous reviewers for constructive remarks. This study was supported by a
616 research agreement between the IFREMER and LODYC institutes, and by the FP6
617 CarboOcean European project. We are indebted to N. Martin for data processing and software
618 development and to O. Coze for handling comparisons of LODYC and IFREMER K grids.
619 We thank T. Takahashi for providing his pCO₂ climatology and for fruitful discussions about
620 oceanic pCO₂ trends. We thank S. Arnault for helpful discussions about altimetry.
621 QuikSCAT K fields are routinely processed and are available on the CERSAT/IFREMER ftp
622 site:

623 <ftp.ifremer.fr>

624 directory: */ifremer/cersat/products/gridded/kco2-quikscat/*

625 Software for reading and collocating K maps with in situ data is available on:

626 <http://www.locean->

627 [ipsl.upmc.fr/index.php?option=com_content&task=view&id=44&Itemid=64](http://www.locean-ipsl.upmc.fr/index.php?option=com_content&task=view&id=44&Itemid=64)

628

629

630 **Table 1 : QuikSCAT-in situ 10m neutral wind speed colocations. Equations of orthogonal regression lines**

Region	Anemometer type	<Uinsitu> (m s-1)	<Uqscat> (m s-1)	Equation of orthogonal fit	95% confidence limit on slope	Rms (y-yfit) (m s-1)	N
North Atlantic	'Debucoart'*	5.99	6.93	$U_{qscat}=1.18 U_{in_situ} - 0.16$	1.16-1.21	0.95	897
North Atlantic	'Vector' cup instrument*	8.33	8.80	$U_{qscat}=1.10 U_{in_situ} - 0.38$	1.07-1.14	1.03	348
Southern Ocean	'Debucoart'*	7.87	9.07	$U_{qscat}=1.20U_{in_situ} - 0.40$	1.16-1.25	0.91	261
Southern Ocean	'Sonic'	8.60	8.99	$U_{qscat}=1.19U_{in_situ} - 1.28$	1.14-1.24	1.02	238

631 *: 2m height in situ wind speeds converted to 10m height wind speeds assuming stable conditions

632

633 **Table 2: Summary of QuikSCAT-in situ 10m neutral wind speed comparisons after correction of possible**
 634 **in situ data biases: CARIOCA-Debu-court wind speeds corrected for possible 8% underestimation; in situ**
 635 **data acquired with Debu-court and ‘Vector’ cup instruments corrected for 0.15m s⁻¹ bias possibly due to**
 636 **atmospheric stability effect.**

Region	Anemometer type	$\langle U_{\text{insitu}} \rangle$ (m s ⁻¹)	σU_{insitu} (m s ⁻¹)	$\langle U_{\text{qscat}} \rangle$ (m s ⁻¹)	σU_{qscat} (m s ⁻¹)	$\frac{\langle U_{\text{qscat}} \rangle}{\langle U_{\text{insitu}} \rangle}$	$\frac{\langle U_{\text{qscat}}^2 \rangle}{\langle U_{\text{insitu}}^2 \rangle}$
North Atlantic	‘Debu-court’	6.6	2.8	6.9	3.1	1.04	1.10
North Atlantic	‘Vector’ cup instrument	8.5	3.3	8.8	3.7	1.04	1.08
Southern Ocean	‘Debu-court’	8.7	2.9	9.1	3.2	1.05	1.12
Southern Ocean	‘Sonic’	8.6	2.9	9.0	3.4	1.05	1.12

637

638

639 **Table 3 : Net Sea-Air CO₂ Flux (in Pg (10¹⁵ g) Carbon / year) deduced from [Takahashi et al., 2002]**
 640 **Δp CO₂ fields and QuikSCAT wind speeds between 1999 and 2006 (this study) with [Wanninkhof, 1992],**
 641 **[Ho et al., 2006] and [Nightingale et al., 2000] k-U relationships. For reference, fluxes available at**
 642 **http://www.ldeo.columbia.edu/res/pi/CO2/carbondioxide/text/10m_wind.prn and computed by**
 643 **Takahashi's group using [Takahashi et al., 2002] Δp CO₂ fields, NCAR/NCEP 41-Year Reanalysis Wind**
 644 **Data at 10 Meter Height, and the long-term Wanninkhof (1992) k-U relationship, K_{WLT} , are also reported.**

645

Lat. Band	Wind speed	K	Pacific	Atlantic	Indian	Southern	All basins
N. of 50°N	QuikSCAT	K_W	0.01	-0.35			-0.35
	QuikSCAT	K_H	0.01	-0.29			-0.30
	QuikSCAT	K_N	0.01	-0.29			-0.29
N. of 50°N	NCEP	K_{WLT}	0.01	-0.31			-0.30
14°N-50°N	QuikSCAT	K_W	-0.54	-0.29	0.05		-0.77
	QuikSCAT	K_H	-0.44	-0.24	0.04		-0.63
	QuikSCAT	K_N	-0.44	-0.23	0.04		-0.63
14°N-50°N	NCEP	K_{WLT}	-0.50	-0.27			-0.72
14°S-14°N	QuikSCAT	K_W	0.74	0.13	0.17		1.04
	QuikSCAT	K_H	0.60	0.11	0.14		0.85
	QuikSCAT	K_N	0.64	0.11	0.14		0.90
14°S-14°N	NCEP	K_{WLT}	0.62	0.12	0.14		0.89
14°S-50°S	QuikSCAT	K_W	-0.37	-0.27	-0.63		-1.27
	QuikSCAT	K_H	-0.30	-0.22	-0.51		-1.04
	QuikSCAT	K_N	-0.30	-0.22	-0.52		-1.04
14°S-50°S	NCEP	K_{WLT}	-0.40	-0.24	-0.52		-1.16
S. of 50°S	QuikSCAT	K_W				-0.41	-0.41
	QuikSCAT	K_H				-0.34	-0.34
	QuikSCAT	K_N				-0.34	-0.34
S. of 50°S	NCEP	K_{WLT}				-0.35	-0.35
Total	QuikSCAT	K_W	-0.16	-0.78	-0.41	-0.41	-1.77
	QuikSCAT	K_H	-0.13	-0.64	-0.33	-0.34	-1.45
	QuikSCAT	K_N	-0.09	-0.63	-0.34	-0.34	-1.39
Total	NCEP	K_{WLT}	-0.27	-0.69	-0.33	-0.35	-1.64

646

647

648

649 **Table A 1:** Colocation periods of QuikSCAT with in situ wind speed

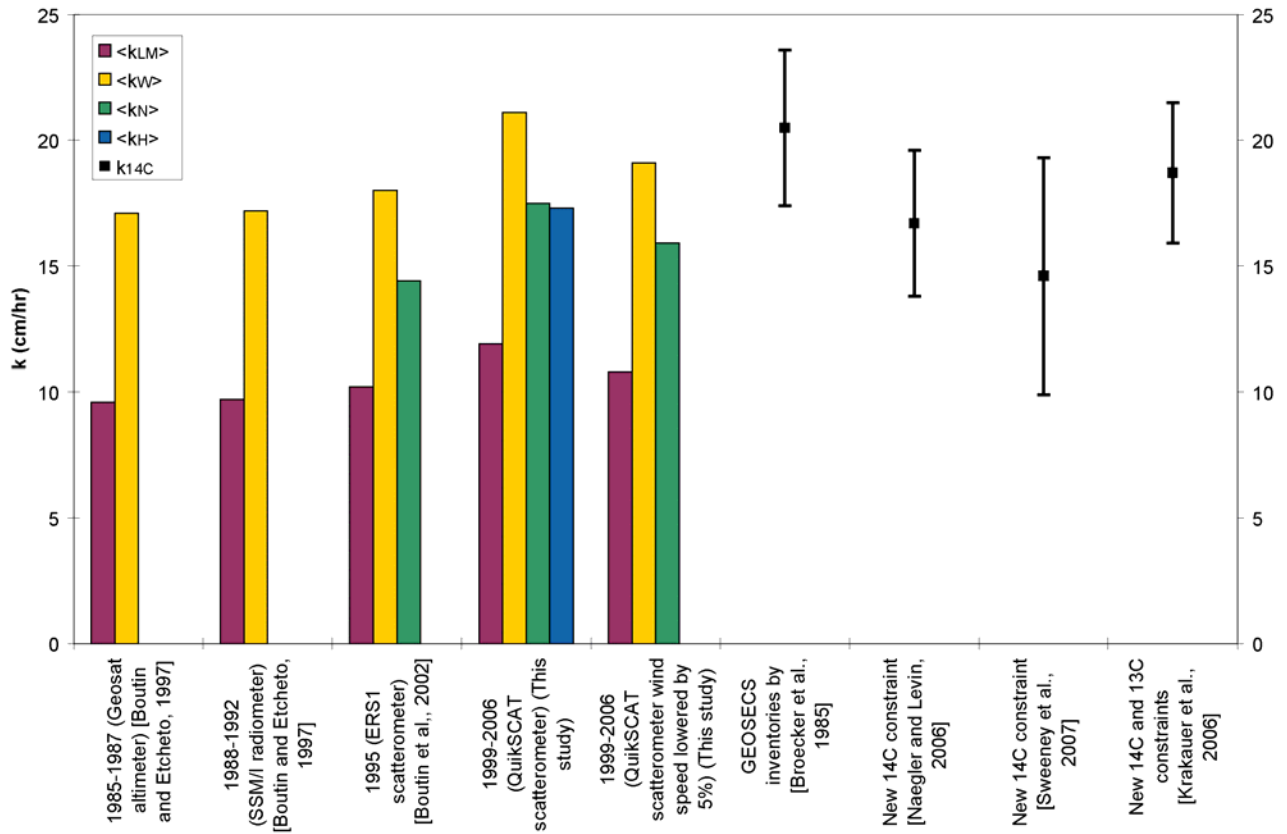
Period of wind measurements	Buoy type – Ocean sector	Anemometer type
09/02/01 to 31/12/01	CARIOCA - North Atlantic	'Debucourt' Cup anemometer
27/08/00 to 03/05/01	Moored buoy - North Atlantic	'Vector' Cup anemometer
20/11/01 to 29/12/01	CARIOCA – Southern Ocean	'Debucourt' Cup anemometer
13/01/02 to 03/03/02	CARIOCA – Southern Ocean	'Debucourt' Cup anemometer
13/01/02 to 13/03/02	CARIOCA – Southern Ocean	'Debucourt' Cup anemometer
30/01/03 to 22/04/03	CARIOCA – Southern Ocean	'Debucourt' Cup anemometer
31/01/06 to 10/07/06	CARIOCA – Southern Ocean	Sonic anemometer

650

651

652

653
654
655

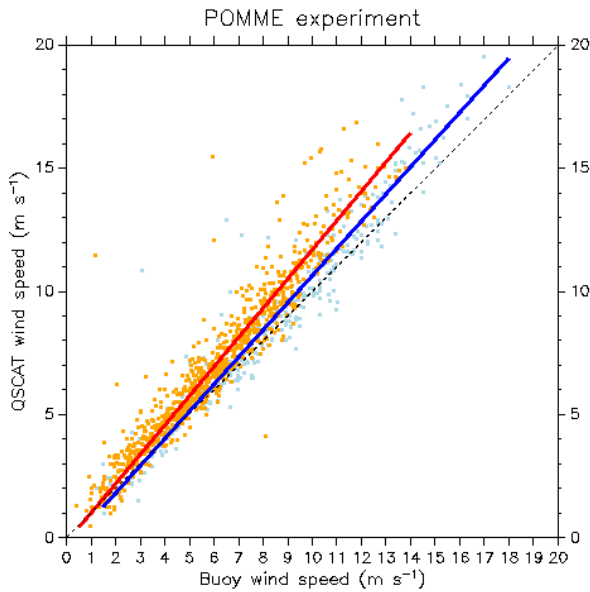


656
657
658
659
660
661
662
663
664
665

Figure 1 : Global averages of k (in cm hr^{-1}) deduced from long time series of satellite wind speeds and k - U relationships (bar charts) (maroon bars: k_{LM} , yellow bars: k_W , green bars: k_N , blue bars: k_H) and deduced from ^{14}C global inventories (black squares) (errors are the ones reported in the original papers). The GEOSECS inventory is the [Wanninkhof, 1992] original value at 20°C converted to in situ SST; the [Naegler and Levin, 2006] estimate is deduced from NCEP, ECMWF, SSMI, QSCAT and ERS2 wind speeds and OPA Ocean General Circulation model; the [Sweeney et al., 2007] estimate is deduced from NCEP wind speeds and three versions of the GFDL MOM3 Ocean General Circulation Model; the original values of [Krakauer et al., 2006] at 20°C were converted to in situ SST (they assume linear k - U relationship and use SSM/I climatological squared wind speed).

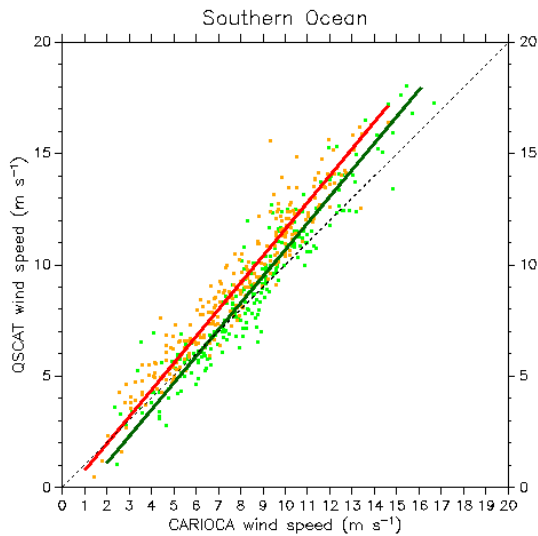
666

QSCAT versus CARIOCA and METEO BUOY 10m wind speed



667

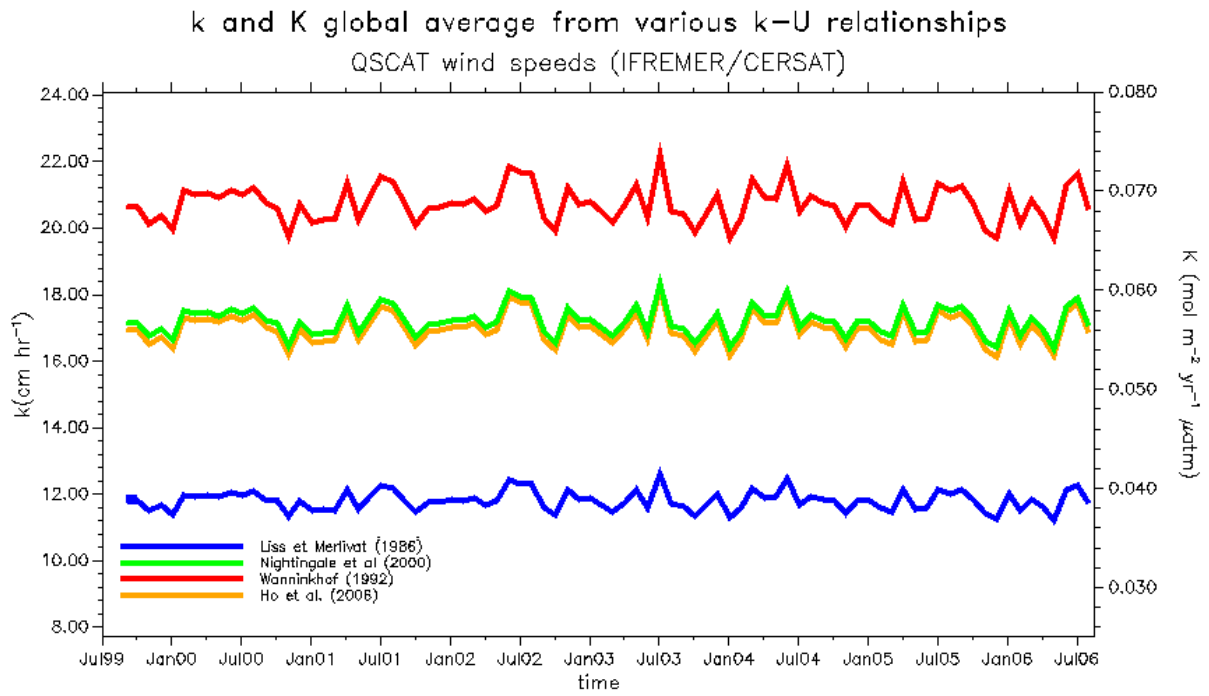
QSCAT and CARIOCA 10m neutral wind speed



668

669

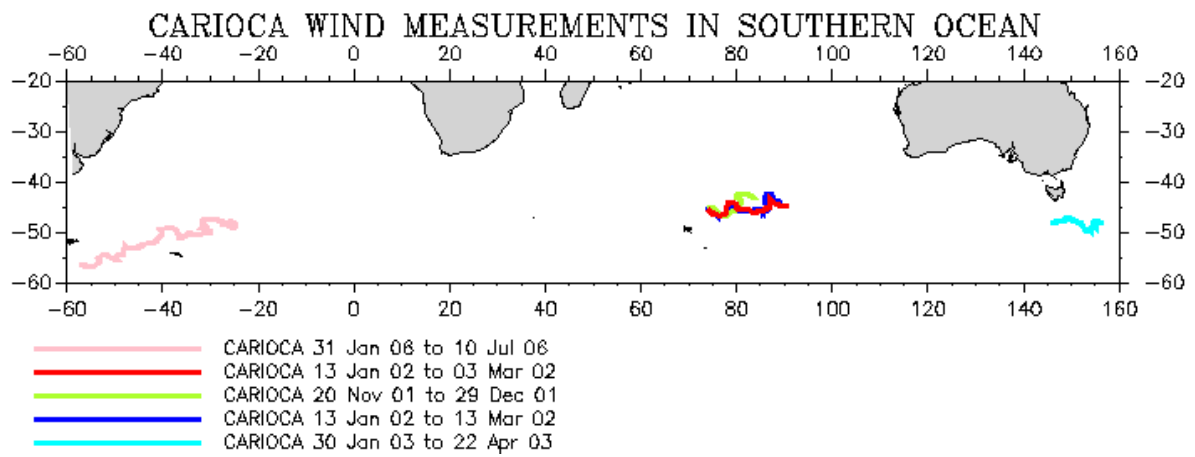
670 **Figure 2 : QuikSCAT wind speed versus 10m in situ wind speed. Statistics of the comparisons are given in**
671 **Table 1. The 1:1 line is indicated as a dashed line. Top) Comparisons in the northern Atlantic during the**
672 **POMME experiment with CARIOCA (Debucoart anemometer) (orange points) and meteorological buoy**
673 **(light blue points) wind speed . Red and blue lines indicate orthogonal regression lines for the CARIOCA-**
674 **QuikSCAT and meteorological buoy-QuikSCAT comparisons respectively. Bottom) CARIOCA wind**
675 **speed in the Southern Ocean. CARIOCA measured with Debucoart anemometer (converted to 10m height**
676 **without correction for atmosphere stability) (orange points) and with Sonic anemometer (converted to**
677 **10m height with correction for atmosphere stability) (green points). Red and green lines indicate**
678 **orthogonal regression lines between QuikSCAT and CARIOCA-Debucoart anemometer wind speeds and**
679 **between QuikSCAT and CARIOCA-Sonic anemometer wind speeds respectively.**



681

682 **Figure 3 : Monthly air-sea CO₂ transfer velocity (left scale) and exchange coefficient (right scale) deduced**
 683 **from QuikSCAT wind speeds from 1999 to 2006 using k-U relationships of Liss and Merlivat (1986)**
 684 **(blue), Nightingale et al. (2000) (green), Ho et al. (2006) (orange) and Wanninkhof (1992) (red) and**
 685 **integrated over the global ocean (80°S-80°N).**

686

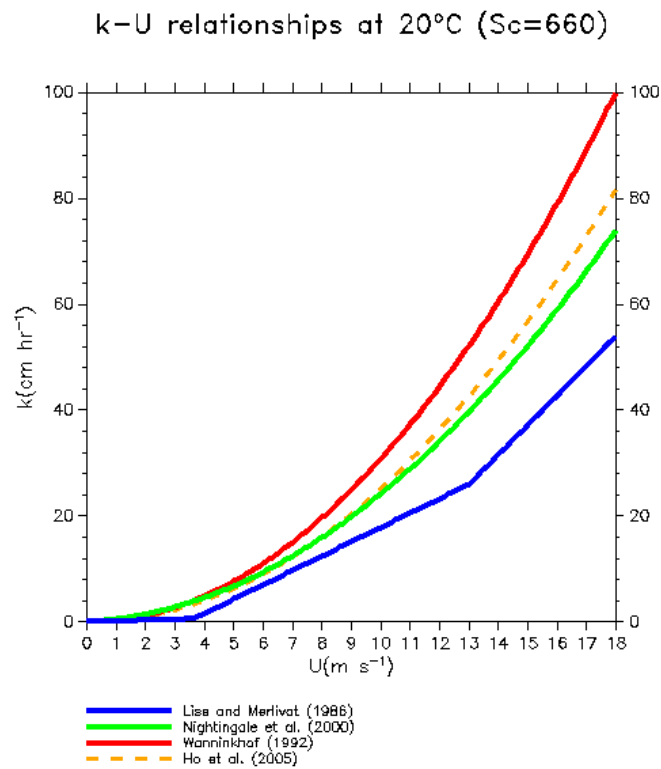


687

688 **Figure A 1: CARIOCA wind speeds location in the Southern ocean**

689

690



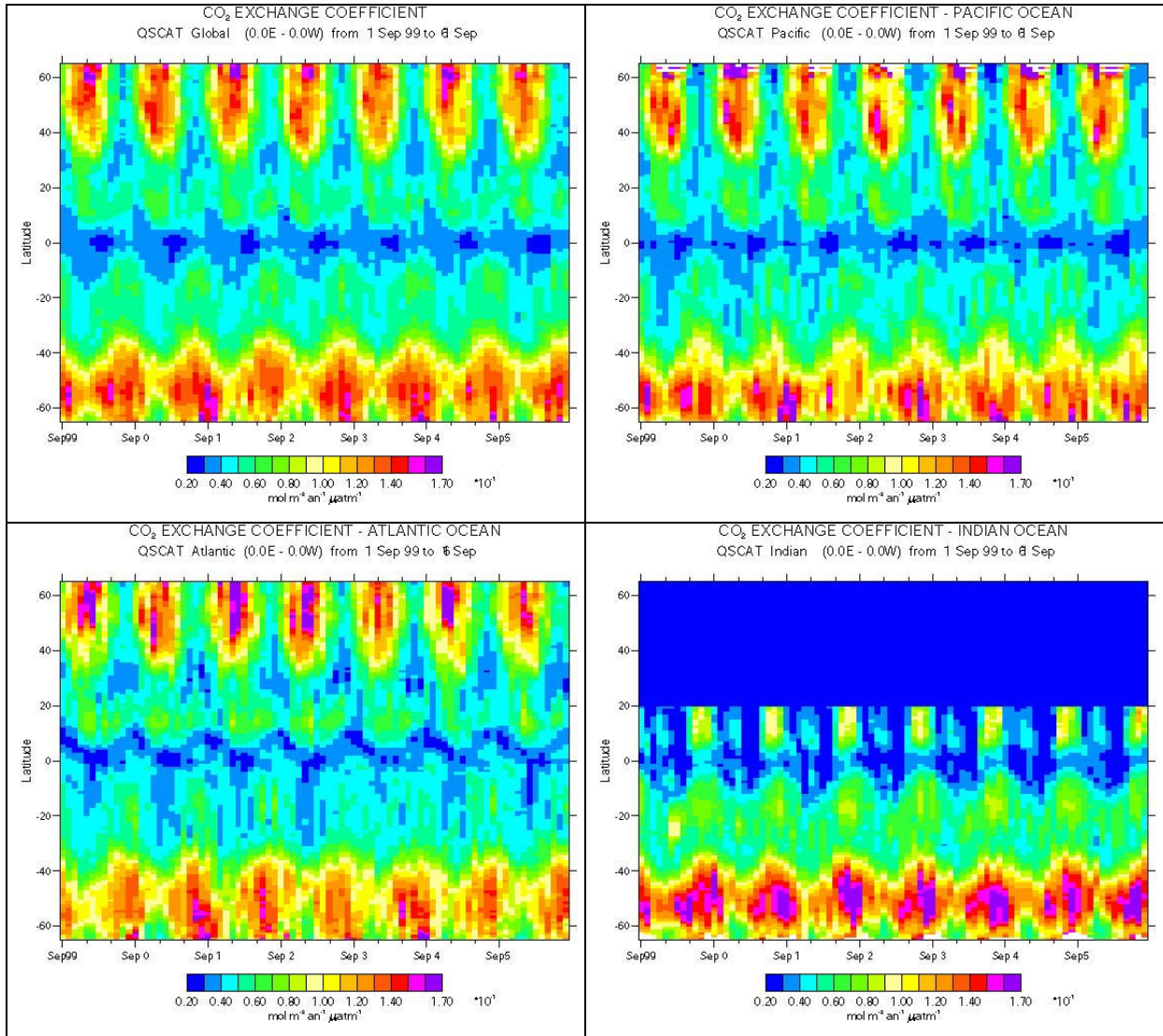
691

692 **Figure B 1:** k-U relationships of [Liss and Merlivat, 1986] (blue), [Nightingale et al., 2000] (green) , [Ho et
693 al., 2006] (orange) and [Wanninkhof, 1992] (red).

694

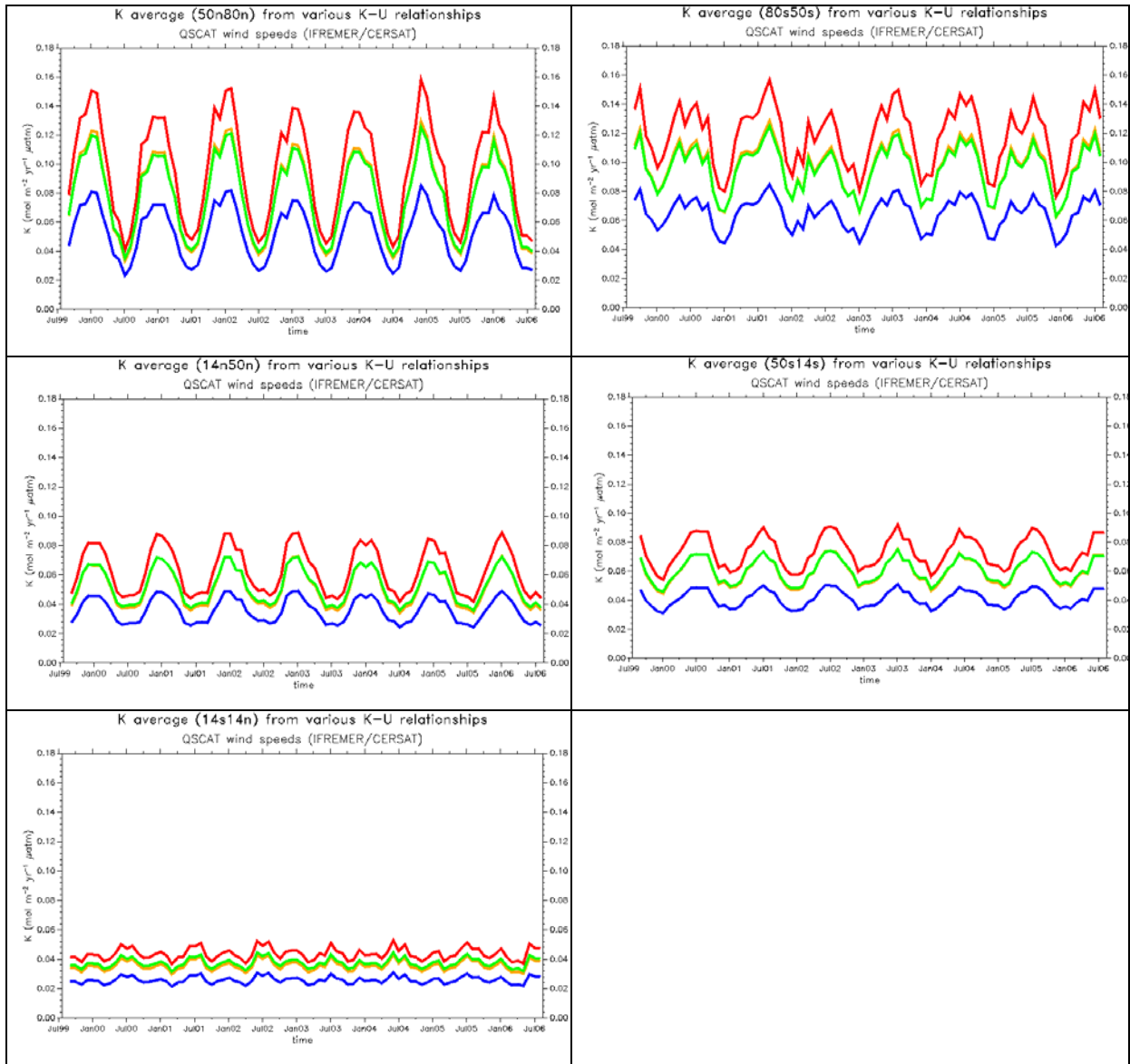
695

696



697

698 **Figure B 2 : Monthly zonal average of K_w from September 1999 to September 2006 derived from**
699 **QuikSCAT wind speeds. top, left) Global Ocean; top, right) Pacific Ocean; bottom, left) Atlantic Ocean;**
700 **bottom, right) Indian Ocean. The same patterns would be obtained for K derived with the [Ho et al.,**
701 **2006] k-U relationship with a color scale ranging from 0.02 to 0.14 mol m⁻² yr⁻¹ μatm⁻¹; this corresponds**
702 **to approximately 5cm hr⁻¹ to 46cm hr⁻¹ for k_{H660} (see text) .**



704

705 **Figure B 3: Monthly CO₂ exchange coefficients deduced from QuikSCAT wind speeds and k-U**
 706 **relationships of Liss and Merlivat (1986) (blue), Nightingale et al. (2000) (green), Ho et al. (2006)**
 707 **(orange), and Wanninkhof (1992) (red) and integrated over latitudinal bands. Top: high latitude:**
 708 **top,right) 50°N-80°N; top, left) 50°S-80°S; middle: mid latitudes: middle, left) 14°N-50°N; middle, right)**
 709 **14°S-50°S; bottom, left) tropics: 14°S-14°N.**

710 **REFERENCES:**

- 711
712 Bakker, D.C.E., J. Etcheto, J. Boutin, and L. Merlivat, Variability of surface-water fCO₂
713 during seasonal upwelling in the equatorial Atlantic Ocean as observed by a drifting
714 buoy, *J. Geophys. Res.*, *106*, 9241-9254, 2001.
- 715 Bentamy, A., and J.F.Piollé, QuikSCAT scatterometer mean wind fields product - User
716 manual - C2-MUT-W-03-IF, IFREMER/CERSAT, Brest, France, 2002.
- 717 Bentamy, A., Y. Quilfen, F. Gohin, N. Grima, M. Lenaour, and J. Servain, Determination and
718 validation of average wind fields from ERS-1 scatterometer measurements, *The*
719 *Global Atmosphere and Ocean System*, *4*, 1-29, 1996.
- 720 Bourassa, M.A., D.M. Legler, J.J. O'Brien, and S.R. Smith, SeaWinds validation with
721 research vessels, *J. Geophys. Res.*, *108 (C2)*, 3019, doi:10.1029/2001JC001028, 2003.
- 722 Boutin, J., and J. Etcheto, Consistency of Geosat, SSM/I and ERS1 global surface wind
723 speeds; comparison with in-situ data, *J. Atmos. Oceanic Technol.*, *13*, 183-197, 1996.
- 724 Boutin, J., and J. Etcheto, Long term variability of the air-sea CO₂ exchange coefficient:
725 Consequences for the CO₂ fluxes in the equatorial Pacific Ocean, *Global Biogeochem.*
726 *Cycles*, *11*, 453-470, 1997.
- 727 Boutin, J., J. Etcheto, Y. Dandonneau, D.C.E. Bakker, R.A. Feely, H.Y. Inoue, M. Ishii, R.D.
728 Ling, P.D. Nightingale, N. Metzl, and R. Wanninkhof, Satellite sea surface
729 temperature: a powerful tool for interpreting in situ pCO₂ measurements in the
730 equatorial Pacific Ocean, *TellusB*, *51B*, 490-508, 1999a.
- 731 Boutin, J., J. Etcheto, L. Merlivat, and Y. Rangama, Influence of gas exchange coefficient
732 parameterization on seasonal and regional variability of CO₂ air-sea fluxes, *Geophys.*
733 *Res. Lett.*, *29/8*, 2002.
- 734 Boutin, J., J. Etcheto, M. Rafizadeh, and D.C.E. Bakker, Comparison of NSCAT, ERS2
735 active microwave instrument, special sensor microwave imager, and Carbon Interface

736 Ocean Atmosphere buoy wind speed: consequences for the air-sea CO₂ exchange
737 coefficient, *J. Geophys. Res.*, *104 (C5)*, 11375-11392, 1999b.

738 Broecker, W.S., T.H. Peng, G. Ostlung, and M. Stuiver, The distribution of bomb radiocarbon
739 in the ocean, *J. Geophys. Res.*, *90*, 6953-6970, 1985.

740 Caniaux, G., A. Brut, D. Bourras, H. Giordani, A. Paci, L. Prieur, and G. Reverdin, A 1 year
741 sea surface heat budget in the northeastern Atlantic basin during the POMME
742 experiment: 1. Flux estimates, *J. Geophys. Res.*, *110*, C07S02,
743 doi:10.1029/2004JC002596, 2005.

744 Carr, M.-E., W. Tang, and W.T. Liu, CO₂ exchange coefficients from remotely sensed wind
745 speed measurements: SSM/I versus QuikSCAT in 2000, *Geophys. Res. Lett.*, *29 (15)*,
746 doi:10.1029/2002GL015068, 2002.

747 Drennan, W.M., P.K. Taylor, and M.J. Yelland, Parameterizing the sea surface roughness, *J.*
748 *Phys. Oceanogr.*, 835-848, 2005.

749 Ebuchi, N., H.C. Graber, and M.J. Caruso, Evaluation of wind vectors observed by
750 QuikSCAT/SeaWinds using ocean buoy data, *J. Atmos. Oceanic Technol.*, *19*, 2049-
751 2062, 2002.

752 Etcheto, J., J. Boutin, Y. Dandonneau, D.C.E. Bakker, R.A. Feely, R.D. Ling, P.D.
753 Nightingale, and R. Wanninkhof, Air-sea CO₂ flux variability in the equatorial Pacific
754 Ocean east of 100°W, *TellusB*, *51B*, 734-747, 1999.

755 Etcheto, J., and L. Merlivat, Satellite determination of the carbon dioxide exchange
756 coefficient at the ocean-atmosphere interface: A first step, *J. Geophys. Res.*, *93*,
757 15669-15678, 1988.

758 Feely, R.A., J. Boutin, C.E. Cosca, Y. Dandonneau, J. Etcheto, H.Y. Inoue, M. Ishii, C.L.
759 Quere, D. Mackey, M.M. Phaden, N. Metzl, A. Poisson, and R. Wanninkhof, Seasonal

760 and Interannual Variability of CO₂ in the equatorial Pacific, *Deep Sea Research Part*
761 *II: Topical Studies in Oceanography*, 49 (13-14), 2443-2469, 2002.

762 Feely, R.A., T. Takahashi, R. Wanninkhof, M.J. McPhaden, C.E. Cosca, S.C. Sutherland, and
763 M. Carr, Decadal variability of the air-sea CO₂ fluxes in the equatorial Pacific Ocean,
764 *J. Geophys. Res.*, 111, C08S90, doi:10.1029/2005JC003129, 2006.

765 Freilich, M.H., and B.A. Vanhoff, The accuracy of preliminary Windsat vector wind
766 measurements: comparison with NDBC buoys and QuikSCAT, *IEEE Trans. Geosci.*
767 *Remote Sens.*, 44 (3), 622-637, 2006.

768 Frew, N.M., E.J. Bock, U. Schimpf, T. Hara, H. Haussecker, J.B. Edson, W.R. McGillis, R.K.
769 Nelson, S.P. McKenna, M.B.M. Uz, and B. Jahne, Air-sea gas transfer: Its dependence
770 on wind stress, small-scale roughness and surface films, *J. Geophys. Res.*, 109,
771 C08S17, doi: 10.1029/2003JC002131, 2004.

772 Frew, N.M., D.M. Glover, E.J. Bock, and S.J. McCue, A new approach to estimation of
773 global air-sea gas transfer velocity fields using dual-frequency altimeter backscatter, *J.*
774 *Geophys. Res.*, 112, C11003, doi:10.1029/2006JC003819, 2007.

775 Glover, D.M., N.M. Frew, and S.J. McCue, Air-sea gas transfer velocity estimates from the
776 Jason-1 and TOPEX altimeters: Prospects for a long-term global time series, *Journal*
777 *of Marine Systems*, 66 (1-4), 173-181, doi:10.1016/j.jmarsys.2006.03.020, 2007.

778 Ho, D.T., C.S. Law, M.J. Smith, P. Schlosser, M. Harvey, and P. Hill, Measurements of air-
779 sea gas exchange at high wind speeds in the Southern Ocean: Implications for global
780 parameterizations, *Geophys. Res. Lett.*, 33, L16611, doi:10.1029/2006GL026817,
781 2006.

782 Hood, E.M., and L. Merlivat, Annual to interannual variations of fCO₂ in the northwestern
783 Mediterranean Sea: high frequency time series data from CARIOCA buoys (1995-
784 1997), *J. Marine Res.*, 59, 113-131, 2001.

785 Kara, A.B., E.J. Metzger, and M.A. Bourassa, Ocean current and wave effects on wind stress
786 drag coefficient over the global ocean, *Geophys. Res. Lett.*, *34*, L01604,
787 doi:10.1029/2006GL027849, 2007.

788 Kelly, K.A., S. Dickinson, M.J. McPhaden, and G.C. Johnson, Ocean currents evident in
789 satellite wind data, *Geophys. Res. Lett.*, *28*, 2469-2472, 2001.

790 Key, R.M., A. Kozyr, C.L. Sabine, K. Lee, R. Wanninkhof, J.L. Bullister, R.A. Feely, J.F.
791 Millero, C. Mordy, and T.H. Peng, A global ocean carbon climatology: Results from
792 Gobal Data Analysis Project (GLODAP), *Global Biogeochem. Cycles*, *18*, GB4031,
793 doi:10.1029/2004GB002247, 2004.

794 Krakauer, N.Y., J.T. Randerson, F.W. Primeau, N. Gruber, and D. Menemenlis, Carbon
795 isotope evidence for the latitudinal distribution and wind speed dependence of the air-
796 sea transfer velocity, *Tellus*, *58B*, 390-417, 2006.

797 Lefèvre, N., J. Aiken, J. Rutllant, G. Daneri, S. Lavender, and T. Smyth, Observations of
798 pCO₂ in the coastal upwelling off Chile: Spatial and temporal extrapolation using
799 satellite data, *J. Geophys. Res.*, *107* (C6), doi:10.1029/2000JC000395, 2002.

800 Liss, P.S., and L. Merlivat, Air-sea gas exchange rates: Introduction and synthesis, in *The*
801 *Role of Air-Sea Exchange in Geochemical Cycling*, edited by P. Buat-Ménart, pp. 113-
802 127, D. Reidel, Norwell, Mass., 1986.

803 Liu, W.T., and W. Tang, Equivalent neutral wind, pp. 8, Jet Propul. Lab., Pasadena, Calif.,
804 1996.

805 Merlivat, L., and P. Brault, CARIOCA Buoy: Carbon Dioxide Monitor, *Sea Technol.*, 23-30,
806 1995.

807 Merlivat, L., M.G. Davila, G. Caniaux, J. Boutin, and G. Reverdin, Mesoscale and diel to
808 monthly variability of CO₂ and carbon fluxes at the ocean surface in the northeastern
809 Atlantic, *J. Geophys. Res.*, *in press*, 2008.

810 Naegler, T., and I. Levin, Closing the global radiocarbon budget 1945–2005, *J. Geophys.*
811 *Res.*, *111*, D12311, doi:10.1029/2005JD006758, 2006.

812 Naegler, T., P. Ciais, K.B. Rodgers, and I. Levin, Excess radiocarbon constraints on air-sea
813 gas exchange and the uptake of CO₂ by the oceans, *Geophys. Res. Lett.*, *33*, L11802,
814 doi:10.1029/2005GL025408., 2006.

815 Nightingale, P.D., G. Malin, C.S. Law, A.J. Watson, P.S. Liss, M.I. Liddicoat, J. Boutin, and
816 R.C. Upstill-Goddard, In-situ evaluation of air-sea gas exchange parameterizations
817 using novel conservative and volatile tracers, *Global Biogeochem. Cycles*, *14*, 373-
818 387, 2000.

819 Olsen, A., R. Waninkhof, J.A. Trinanes, and T. Johannessen, The effect of wind speed
820 products and wind speed–gas exchange relationships on interannual variability of the
821 air–sea CO₂ gas transfer velocity, *Tellus B*, *57* (2), 95-106, 2005.

822 Peacock, S., Debate over the ocean bomb radiocarbon sink: Closing the gap, *Global*
823 *Biogeochem. Cycles*, *18*, GB2022, doi:10.1029/2003GB002211, 2004.

824 Queffeuilou, P., S. Didailier, R. Ezraty, A. Bentamy, and J.P. Gouillou, Toscane 2 Campaign
825 report - Ifremer contribution, 1988.

826 Quilfen, Y., B. Chapron, and V. Vandemark, The ERS scatterometer wind measurement
827 accuracy: Evidence of seasonal and regional biases, *J. Atmos. Oceanic Technol.*, *18*,
828 1684-1697, 2001.

829 Quilfen, Y., C. Prigent, B. Chapron, A.A. Mouche, and N. Houtin, The potential of
830 QuikSCAT and WindSat observations for the estimations of sea surface wind vector
831 under severe weather conditions, *J. Geophys. Res.*, *112*, C09023,
832 doi:10.1029/2007JC004163, 2007.

833 Rangama, Y., J. Boutin, J. Etcheto, L. Merlivat, T. Takahashi, B. Delille, M. Frankignoulle,
834 and D.C.E. Bakker, Variability of net air-sea CO₂ flux inferred from in-situ and

835 satellite measurements in the Southern Ocean south of Tasmania and New Zealand, *J.*
836 *Geophys. Res.*, *110*, C09005, doi 10.1029/2004JC002619, 2005.

837 Reynolds, R.W., N.A. Rayner, T.M. Smith, D.C. Stokes, and W. Wang, An Improved In Situ
838 and Satellite SST Analysis for Climate, *J. Climate*, *15*, 1609-1625, 2002.

839 Sabine, C.L., R.A. Feely, N. Gruber, R.M. Key, K. Lee, J.L. Bullister, R. Wanninkhof, C.S.
840 Wong, D.W.R. Wallace, B. Tilbrook, F.J. Millero, T.-H. Peng, A. Kozyr, T. Onon,
841 and A.F. Rios, The oceanic sink for anthropogenic CO₂, *Science*, *305*, 367-371, 2004.

842 Sweeney, C., E. Gloor, A.R. Jacobson, R.M. Key, G. McKinley, J.L. Sarmiento, and R.
843 Wanninkhof, Constraining global air-sea gas exchange for CO₂ with recent bomb ¹⁴C
844 measurements, *Global Biogeochem. Cycles*, *21*, GB2015,
845 doi:10.1029/2006GB002784, 2007.

846 Takahashi, T., S.C. Sutherland, C. Sweeney, A. Poisson, N. Metzl, B. Tilbrook, N. Bates, R.
847 Wanninkhof, R.A. Feely, C. Sabine, J. Olafsson, and Y. Nojiri, Global sea-air CO₂
848 flux based on climatological surface ocean pCO₂ and seasonal biological and
849 temperature effects, *Deep Sea Research Part II*, *49* (9-10), 1601-1622, 2002.

850 Wanninkhof, R., Relationship between wind speed and gas exchange over the ocean, *J.*
851 *Geophys. Res.*, *97*, 7373-7382, 1992.

852 Wanninkhof, R., The impact of different gas exchange formulations and wind speed products
853 on global air-sea CO₂ fluxes, in *Transport at the air sea interface*, edited by C.S.
854 Garbe, R.A. Handler, B. Jähne, pp. 1-23, Springer-Verlag Berlin, Heidelberg, 2007.

855 Wanninkhof, R., S.C. Doney, T. Takahashi, and W.R. McGillis, The effect of using time-
856 averaged winds on regional air-sea CO₂ fluxes, in *Gas Transfer at Water Surfaces*,
857 edited by M.A. Donelan, W. M. Drennan, E. S. Saltzman and R. Wanninkhof, pp.
858 351-356, American Union Geophysical Monograph 127, AGU, Washington, DC,
859 2002.

860 Weiss, R.F., Carbon dioxide in water and seawater: The solubility of a nonideal gas, *Mar.*
861 *Chem.*, 2, 203-215, 1974.

862

863